

Ice stratigraphy at the Pâkitsoq ice margin, West Greenland, derived from gas records

Hinrich SCHAEFER,^{1*} Vasilii V. PETRENKO,^{2†} Edward J. BROOK,¹
Jeffrey P. SEVERINGHAUS,² Niels REEH,^{3‡} Joe R. MELTON,⁴ Logan MITCHELL¹

¹Department of Geosciences, Oregon State University, Corvallis, Oregon 97331-5506, USA

E-mail: h.schaefer@niwa.co.nz

²Scripps Institution of Oceanography, University of California San Diego, La Jolla, California 92093-0225, USA

³National Space Institute, Technical University of Denmark, Building 348, Ørstedes Plads, DK-2800 Kgs Lyngby, Denmark

⁴School of Earth and Ocean Sciences, University of Victoria, PO Box 3055, Victoria, British Columbia V8W 3P6, Canada

ABSTRACT. Horizontal ice-core sites, where ancient ice is exposed at the glacier surface, offer unique opportunities for paleo-studies of trace components requiring large sample volumes. Following previous work at the Pâkitsoq ice margin in West Greenland, we use a combination of geochemical parameters measured in the ice matrix ($\delta^{18}\text{O}_{\text{ice}}$) and air occlusions ($\delta^{18}\text{O}_{\text{atm}}$, $\delta^{15}\text{N}$ of N_2 and methane concentration) to date ice layers from specific climatic intervals. The data presented here expand our understanding of the stratigraphy and three-dimensional structure of ice layers outcropping at Pâkitsoq. Sections containing ice from every distinct climatic interval during Termination I, including Last Glacial Maximum, Bølling/Allerød, Younger Dryas and the early Holocene, are identified. In the early Holocene, we find evidence for climatic fluctuations similar to signals found in deep ice cores from Greenland. A second glacial–interglacial transition exposed at the extreme margin of the ice is identified as another outcrop of Termination I (rather than the onset of the Eemian interglacial as postulated in earlier work). Consequently, the main structural feature at Pâkitsoq is a large-scale anticline with accordion-type folding in both exposed sequences of the glacial–Holocene transition, leading to multiple layer duplications and age reversals.

INTRODUCTION

Air occlusions in polar ice offer the only means for direct studies of past changes in atmospheric composition, which are essential for understanding natural climate variability as well as climatic impacts of anthropogenic emissions. Analyses of trace components in air bubbles and the ice matrix are often precluded by the limited availability of ancient ice from deep ice cores. In contrast, at certain ice-margin locations ice flow and bedrock topography fortuitously combine to expose ancient ice layers, offering practically unlimited sample availability. Several such outcrops have been identified in Greenland and Antarctica (Wilch and others, 1999; Reeh and others, 2002; Petrenko and others, 2006; Aciego and others, 2007). These horizontal ice-core sites offer unique opportunities for paleo-environmental studies at lower logistical cost than deep ice-coring projects, but they also pose specific challenges.

The first challenge is age control. Similar to ice cores, where age increases with core depth, in an outcropping ice profile age generally increases along the ice–flow direction, i.e. towards the ice-sheet margin (Reeh and others, 2002). However, deformation at margin settings can lead to non-uniform thinning, folding and even reversal of the sequence with duplication of layers, which complicates dating. Therefore, absolute ages of the ice and occluded air must be derived by comparison of geochemical tracers with deep

ice-core records. Characteristic changes in the tracers at climatic transitions provide stratigraphic anchor points; in between those points ages must be interpolated.

The second challenge is the preservation of paleo-signals. Ice from margin sites has been subject to long-distance transport and deformation, which may alter paleo-signals through: (1) fracturing and meltwater addition (refreezing) from surface and basal melt, which may affect the $^{18}\text{O}/^{16}\text{O}$ signature of the ice matrix ($\delta^{18}\text{O}_{\text{ice}}$) as well as gas composition through the addition of dissolved gases; (2) entrainment of silt particles from basal layers that may host or fuel microbial activity (e.g. Souchez and others, 1995; Price, 2007); (3) exposure to elevated temperatures close to bedrock and at the surface, which increases rates of chemical reactions and metabolic activity; (4) thermal contraction and resulting fracturing in the ablation zone leading to addition of extraneous air; and (5) downward migration of low-albedo surface silt particles and aggregates through radiation-induced melting.

Reeh and Thomsen (1994) and Reeh and others (1991, 1993, 2002) used $\delta^{18}\text{O}_{\text{ice}}$ measurements to show that pre-Holocene ice outcrops at Pâkitsoq at the western margin of the Greenland ice sheet. Later work showed that Pâkitsoq ice can also yield reliable gas records (Petrenko and others, 2006). The study uniquely identified ice dating to the Last Glacial Maximum (LGM), Oldest Dryas (OD), Bølling/Allerød (B/A), Younger Dryas (YD) and Preboreal (PB) climatic intervals and provided the foundation for studies of the Late-glacial methane cycle using the ^{13}C and ^{14}C isotopic signatures (Schaefer and others, 2006; Petrenko, 2008; Petrenko and others, 2009). In this study, we use the same combination of geochemical tracers extracted from the ice to further examine the ice stratigraphy at Pâkitsoq.

*Present address: National Institute of Water and Atmospheric Research Ltd, Private Bag 14901, Kilbirnie, Wellington 6241, New Zealand.

†Present address: Institute of Arctic and Alpine Research, University of Colorado Boulder, Colorado 80309-0450, USA.

‡Deceased.

Table 1. Characteristic values of geochemical parameters for climatic periods at the end of the last ice age as measured in GISP2

	$\delta^{18}\text{O}_{\text{ice}}^*$	$[\text{CH}_4]^\dagger$	$\delta^{18}\text{O}_{\text{atm}}^\ddagger$	$\delta^{15}\text{N}$ excursion [§]
	‰	ppb	‰	‰
Last Glacial Maximum (~18 ka BP)	-40 to -41	350–450	1.1–1.0	
Bølling/Allerød (~12.6–14.7 ka BP)	-36 to -38	600–700	1.0–0.8	+0.16 (0.48–0.64) [¶]
Younger Dryas (~11.6–12.6 ka BP)	-40 to -41	500–550	0.7–0.6	
Preboreal (<11.5 ka BP)	>-38	670–750	≤0.6	+0.16 (0.40–0.56)

*From Grootes and Stuiver (1997).

†From Brook and others (2000).

‡From Bender and others (1994, 1999); here adjusted to account for gas loss fractionation.

§As associated with the warming at the onset of the respective time period.

¶From Severinghaus and Brook (1999).

||From Severinghaus and others (1998).

The ratio of ^{15}N to ^{14}N in trapped air in ice ($\delta^{15}\text{N}$), reported in the δ -notation relative to modern atmospheric N_2 , is a sensitive indicator of rapid atmospheric temperature changes in the past, because the isotopes are fractionated along temperature gradients that develop within the firn column. Consequently, the OD–Bølling and YD–PB abrupt warming events leave large and distinct $\delta^{15}\text{N}$ signals (Severinghaus and others, 1998; Severinghaus and Brook, 1999). Because N_2 is very abundant and chemically inert, this is a very robust tracer insensitive to secondary alteration.

The isotope ratio $^{18}\text{O}/^{16}\text{O}$ of paleo-atmospheric O_2 ($\delta^{18}\text{O}_{\text{atm}}$, reported relative to modern atmospheric O_2 and corrected for gravitational and thermal fractionation in the firn) is affected by global ice volume and biogeochemistry (Bender and others, 1994). Because the atmosphere is well mixed on the millennial timescale of O_2 turnover, all locations on the surface of the Earth (and therefore all ice cores) should experience the same $\delta^{18}\text{O}_{\text{atm}}$ history. With its near-monotonic decrease during the last deglaciation, $\delta^{18}\text{O}_{\text{atm}}$ is distinct at each climatic interval, providing a chronostratigraphic tool (Table 1; Bender and others, 1999).

Atmospheric methane concentration $[\text{CH}_4]$ is a near-global signal (interhemispheric gradient is $\leq 10\%$) and changes in close unison with Greenland climate (e.g. Severinghaus and others, 1998; Severinghaus and Brook, 1999; Brook and others, 2000). It has characteristic values for each climatic interval with rapid transitions between them, and can be measured in the field to determine immediately and accurately the ice stratigraphy during each sampling season. Unfortunately, some ice sections at Pâkitsoq contain elevated $[\text{CH}_4]$ and care has to be taken to avoid this contaminated ice (Petrenko and others, 2006). We find that slight $[\text{CH}_4]$ elevation (tens of ppb) occurs predominantly in near-surface ice or is associated with a melt signature in the noble gas composition; moderate elevation (up to several hundred ppb) is associated with visible mineral or organic inclusions. In two cases, extreme values that exceed the calibration range of the gas chromatographic analysis (thousands of ppb) were also observed. A more detailed discussion of gas-record alteration in Pâkitsoq ice will be provided elsewhere by Schaefer and others.

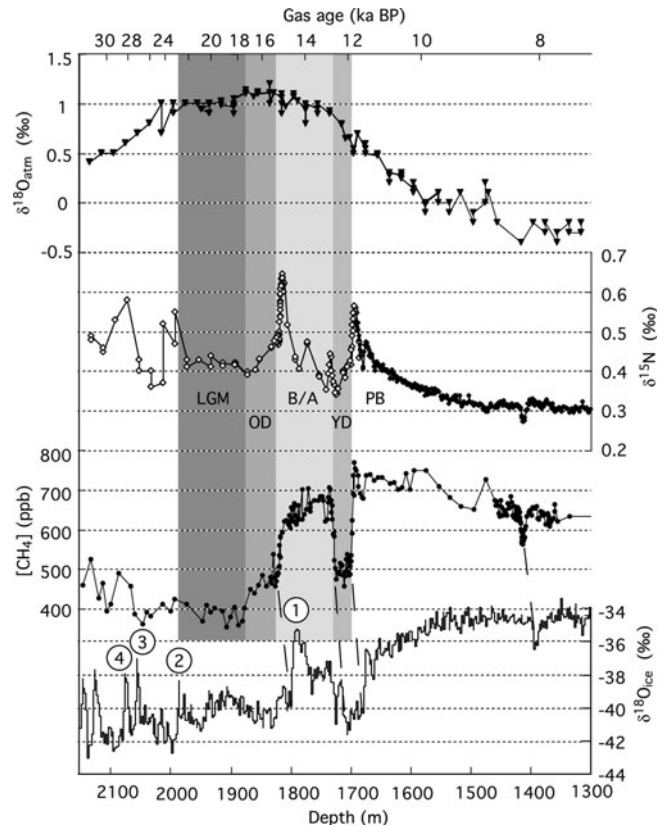


Fig. 1. GISP2 data of geochemical parameters over the last glacial termination. Distinct climatic periods are characterized by the combination of values in $\delta^{18}\text{O}_{\text{atm}}$ (Bender and others, 1999), $[\text{CH}_4]$ (Brook and others, 2000) and $\delta^{18}\text{O}_{\text{ice}}$ (Grootes and Stuiver, 1997). Excursions in $\delta^{15}\text{N}$ mark abrupt warming events (open diamonds: Severinghaus and others, 1998; Severinghaus and Brook, 1999; solid diamonds: Kobashi and others, 2008). These values are used to derive the stratigraphy at Pâkitsoq. All parameters are plotted against depth. Additionally, the top axis gives the gas-age scale from Brook and others (2000), which applies to the three gas records (see shaded boxes for climatic intervals), but not $\delta^{18}\text{O}_{\text{ice}}$ due to the gas-age–ice-age difference (see text). The gas-age–ice-age offset is evident as lateral offset between coeval climatic transitions recorded in $\delta^{18}\text{O}_{\text{ice}}$ and the gas records (see dashed lines that link climate events between $\delta^{18}\text{O}_{\text{ice}}$ and $[\text{CH}_4]$). Circled numbers 1–4 indicate the four youngest Dansgaard–Oeschger events.

$\delta^{18}\text{O}_{\text{ice}}$, which is quite insensitive to contamination because of its large abundance (although melt layers must be avoided), has characteristic values for the different climatic intervals. This provides an age constraint for the ice that is offset from the age of occluded air, which is trapped at the base of the firn layer and is therefore younger than the surrounding ice (e.g. Schwander and others, 1997). This ice-age–gas-age offset can be used to identify stratigraphic disturbances where ice and gas geochemistry change at the exact same location, namely the discontinuity that juxtaposes ice from different climatic intervals. In contrast, for real climate transitions ice and gas tracer changes are spatially separated as a result of the age offset (Landais and others, 2004).

All these tracers are compared with the records measured in the Greenland Ice Sheet Project 2 (GISP2) ice core, which show characteristic values for the climatic intervals and transitions during the last glacial termination (Table 1; Fig. 1). GISP2 is an excellent reference for our records because an ice-sheet flowline model (Reeh and others,

2002) predicts that Pâkitsoq ice from the last glacial termination originates ~ 190 km south and ~ 70 km west of Greenland Summit, i.e. near the GISP2 drill site. A study of the evolution of the three-dimensional ice stratigraphy in the period 1985–2005 based on global positioning system (GPS) mapping, $\delta^{18}\text{O}_{\text{ice}}$ profiles and kinematic modeling is in progress and will be reported elsewhere by Reeh and others.

In this paper, we improve our understanding of the exposed Pâkitsoq ice stratigraphy and ice tectonic patterns by refining and expanding existing profiles. We search for new targets for paleo-studies (e.g. during the early Holocene (EH), such as the 8.2k event (Alley and others, 1997), an interval of widespread cooling centered at 8.2 ka BP (present = AD 1950)). We also investigate an ice layer with $\delta^{18}\text{O}_{\text{ice}}$ values and a surface appearance indicative of interglacial ice in immediate proximity to the ice margin where we suspected the ice to date to the Eemian interval or marine isotopic stage 5e (Reeh and others, 1991), a time period of great interest that is not well sampled by existing ice cores in Greenland.

STUDY AREA AND METHODS

The Pâkitsoq ice margin site ($69^{\circ}25.83' \text{N}$, $50^{\circ}15.20' \text{W}$; Fig. 2) in West Greenland has been described in detail by Reeh and others (1991, 1993, 2002), Reeh and Thomsen (1994) and Petrenko and others (2006). The main topographic feature of the area is a ~ 3 km long northeast–southwest trending mountain ridge that blocks the ice flow in a zone of stagnation and compression, forcing pre-Holocene ice layers upwards to become exposed (Fig. 2). At the sampling area, the ice layers dip southeast at 50 – 70° (Petrenko and others, 2006). The ablation rate is 2 – 3 m a^{-1} . Features in the ice that have been described previously include: (1) horizons with high sediment content ('dust bands'); (2) bubble-free 'blue bands' that range in thickness from millimeters to meters and are interpreted as subglacial meltwater refrozen in cracks; and (3) folding on scales from millimeters to tens of meters (Petrenko and others, 2006).

Ice sampling during the 2004 and 2005 summer field seasons, yielding the results presented here, was conducted largely as described by Petrenko and others (2006) for the 2001–03 campaigns. Briefly, the sampling profile lines were oriented perpendicular to ice stratigraphy (and the ice margin), trending southeast to northwest. Positions of profiles from different years were correlated using 6 m long aluminum poles left as markers in the ice. All distances are reported relative to a marker pole set in 2002, with distances increasing towards the northwest (Table 2; Fig. 3). The exception to this system is the margin profile (PK05 MA), which uses its own distance scale relative to an arbitrary origin with distances increasing towards the southeast (for practical reasons relevant at the time of sampling). Oil-free electrical chainsaws were used to remove the top 20–30 cm of ice to avoid surface contamination. Small sample cores (~ 100 g), used for all gas analyses, were taken with an aluminum coring device driven by an electrical hand-held drill (known as the 'Chipmunk', developed by Ice Coring and Drilling Services, Madison, WI, USA). The 2005 campaign lasted from 11 June to 22 July, i.e. earlier in the season than all previous campaigns (2001: 25 August–3 September; 2002: 31 July–13 August; 2003: 15 July–12 August; 2004: 12 July–16 August). All profiles taken in 2004 and 2005 are listed in Table 2 and shown in Figures 2 and 3.

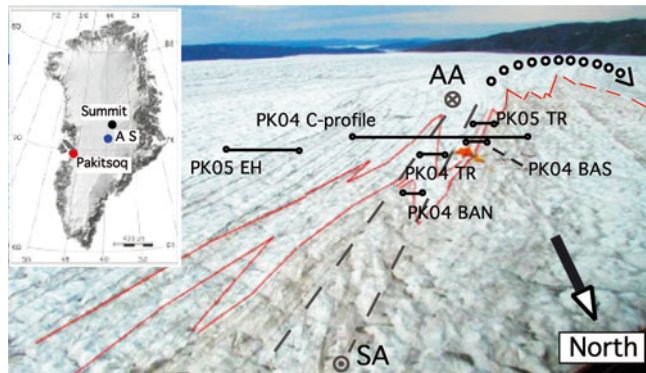


Fig. 2. Oblique aerial photograph of the study site in 2004, looking to the southwest. The orange laboratory tent (10 m long) just below the 2004 C-profile provides a scale. For clarity, some, but not all, 2004 and 2005 gas transects are shown (for positions of all profiles see Fig. 3). Grey dashed lines mark the syncline axis (SA) and anticline axis (AA). Dust bands (thin brown bands) reveal folding tectonic features, which are also visible in the patterns of dark (cold period) and light (warm period) ice. The dotted arrow outlines a broad anticline fold, in which Holocene ice wraps around layers from the last glacial period. Note that here the area is seen from the north, so that the view is rotated relative to the map view of Figure 3. Inset shows the positions of Greenland Summit (black dot; the GISP2 drill site is situated ~ 30 km to the west), Pâkitsoq (red dot) and the Pâkitsoq accumulation site (A S; blue dot) (after Petrenko and others, 2006).

The analytical methods for measurements of $\delta^{18}\text{O}_{\text{atm}}$ and $\delta^{15}\text{N}$ (Scripps Institution of Oceanography, SIO), methane concentration (both in the field and at Oregon State University, OSU), and $\delta^{18}\text{O}_{\text{ice}}$ (University of Copenhagen) have been described in detail by Reeh and others (2002), Petrenko and others (2006) and Schaefer and others (2006). The few procedural differences are as follows. For $\delta^{18}\text{O}_{\text{atm}}$ and $\delta^{15}\text{N}$ analyses, a Finnigan Delta-V dual dynamic inlet mass spectrometer was used for the following samples: all PK04 TR and PK05 TR profiles, PK05 EH, PK05 LGM and PK05 YD. For PK04 BAS, PK04 BAN, PK04 C and PK05 MA profiles, a Finnigan Delta-XP mass spectrometer was used. The gas chromatograph inlet system used for $[\text{CH}_4]$ analysis in the field and laboratory was equipped with a manifold for the simultaneous processing of 12 (previously 6) samples. At OSU, select samples were also measured with an improved apparatus that features knife-edge seals on Cu gaskets for the flasks, a colder ethanol bath ($\sim -60^{\circ}\text{C}$ vs $\sim -30^{\circ}\text{C}$) and an Agilent gas chromatograph. Measurements using the standard methane system and the improved system agreed within the range of uncertainty.

RESULTS AND DISCUSSION

A complete and multiply folded sequence spanning the last glacial termination

At Pâkitsoq the age of the ice layers is expected to increase along the flowline from the southeast to the northwest (Reeh and others, 2002). The transition between Holocene ice and ice from the last glacial period is marked by changes in surface appearance: higher dust content, lack of cryoconite holes and darker ice color characterize the glacial section (Fig. 2). The darker color may be due to: (1) the dust; (2) smaller grain size of the glacial period ice; (3) a lack of redistribution of dust into cryoconite holes that hide it from

Table 2. List of sample profiles

Profile	Depth below ice surface m	Distance along age axis* m	Profile offset along strike† m	Time intervals	Analyzed for				Documented in‡
					[CH ₄]	δ ¹⁵ N	δ ¹⁸ O _{atm}	δ ¹⁸ O _{ice}	
PK04 BAN	0.2–0.4	~2.3 m long	–38.5	OD–BA	X	X	X	X	Fig. 6
PK04 B-profile	0.0–0.1	–25 to 25	–1	TI (mf) [§]				X	
PK04 TR	0.3–0.9	1.1 to 4.1	–1	BA–YD–PB	X	X	X	X	Figs 4 and 5
PK04 BAS	0.2–0.3	15.4 to 17.7	13	OD–BA	X	X	X	X	Figs 4 and 5
PK04 C-profile	0.1–0.2	–21 to 20	13	TI (mf)	X			X	Fig. 4
PK05 C-profile	0.0–0.1	125 m long	~–11	TI (mf)				X	Fig 9
PK05 EH	0.2	24 m long	~–11	EH (~9–10 ka BP)	X	X	X	X	Fig. 9
PK05 TR 2	1.0	14.4 to 15.7	4.6 ± 0.5	OD–BA	X	X	X		Fig. 6
PK05 TR and LGM	1.1	13.7 to 19.8	22.6	LGM–OD–BA	X	X	X	X	Figs 4 and 6
PK05 YD	>0.4	0.9 to 2.5	~20	BA–YD–PB	X	X	X		Figs 4 and 5
PK05 TR 4 Top	~0.2	14.4 to 15.9	33.3	OD–BA	X	X	X		Fig. 6
PK05 TR 4 bottom	1.5	14.2 to 15.5	33.3	OD–BA	X	X	X		Fig. 6
PK05 MA (Eem)	0.2–0.3	57.5 m long		TI (mf)	X	X	X	X	Fig. 7

*Given for profiles in the main study area relative to a reference pole set in 2002 (PK02 RP) (Fig. 3); distances increase towards northwest. For profiles outside the main study area, total length is given.

†Relative to PK02 RP, offset increases towards southwest.

‡All profile positions shown in Figure 3, some also in Figure 2.

§Termination I, multiply folded.

view; and (4) growth of photosynthetic algae stimulated by dust, giving the ice a reddish tint. Profiles of δ¹⁸O_{ice} show that a drop from typical interglacial (~–32‰) to glacial values (~–40‰) (Table 1) marks the transition (e.g. Fig. 4, at 13–17 m). Within the glacial period section Reeh and others (2002) found large δ¹⁸O_{ice} fluctuations that are typical for interstadial events as recorded in the GISP2 ice core (Grootes and Stuiver, 1997). However, the ages of the ice layers, or whether they are in correct stratigraphic order, cannot be deduced from δ¹⁸O_{ice} alone.

Structural geology predicts that isochrons will be repeated three times in an overturned isoclinal fold

comprising a syncline–anticline pair: once on the upright limb of the syncline, once on the overturned limb, and once again on the upright limb of the anticline. In their figure 8, Petrenko and others (2006) used the unique combination of δ¹⁸O_{atm}, [CH₄] and δ¹⁸O_{ice} values for each climatic interval (Fig. 1; Table 1), as well as characteristic excursions in δ¹⁵N, to determine the ages within the main study transect by comparing these records with corresponding records from the deglacial section of the GISP2 ice core. They concluded that the intensely studied section ~500 m from the margin does consist of a syncline–anticline pair with a complete sequence from LGM (~20 ka BP) at the northwestern end to

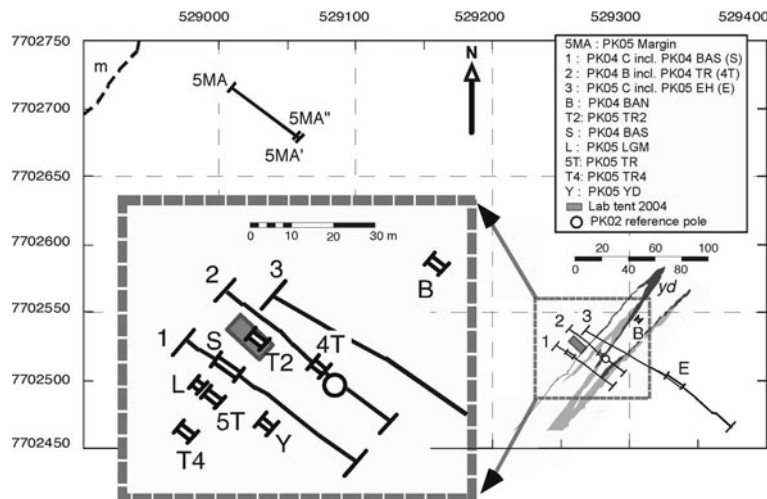


Fig. 3. Map of profiles taken in field seasons 2004 and 2005. Dashed curve indicates approximately the boundary between exposed and moraine-covered (m) ice. Dark grey shading indicates the 2004 surface expression of YD aged ice in the syncline/anticline structure (yd) as mapped using δ¹⁸O_{ice} profiles and an ice-flow model; details will be presented in a forthcoming paper by Reeh and others. Short gas profiles are plotted as double black lines to distinguish them from longer δ¹⁸O_{ice} profiles (single black lines) that overlap in some cases. Length of short gas profiles is in some cases plotted approximately. Inset shows the main study area in more detail, including profiles that are omitted in the main map for clarity. 5MA' and 5MA'' indicate slightly offset end-points of the PK05 MA profiles for gases and δ¹⁸O_{ice}, respectively.

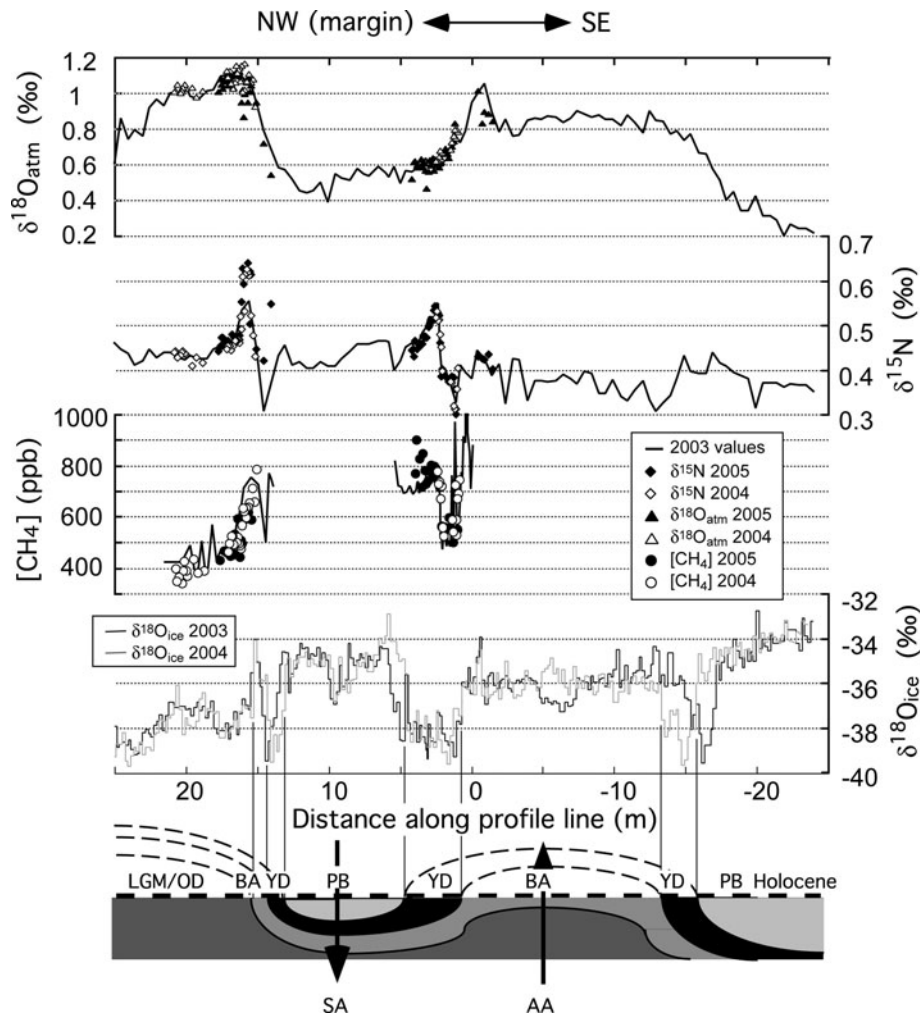


Fig. 4. $\delta^{18}\text{O}_{\text{ice}}$ profiles and gas records spanning climatic transitions in the main study area. Current results are shown in comparison with earlier records (2001–03) (Petrenko and others, 2006). The LGM to B/A sequence of the gas records (at ~ 15 – 20 m, PK04 BAS, as well as PK05 TR and LGM) shows increasing age towards the margin (to northwest), whereas the B/A to YD to PB sequence (at ~ 0 – 5 m, PK04 TR and PK05 YD) is reversed and increases in age away from the margin (to southeast). $[\text{CH}_4]$ results from the long shallow surface profile (PK04 C-profile) are not shown because most values were elevated above contemporary GISP2 values (up to 1400 ppb). The 2004 $\delta^{18}\text{O}_{\text{ice}}$ record is from PK04 C-profile. An offset of -1.4 m was applied to the 2004 profiles to achieve the best match of $\delta^{15}\text{N}$ peaks. The cartoon at the bottom illustrates schematically the folding of the ice layers and indicates approximate positions of syncline axis (SA) and anticline axis (AA), as well as age of surface ice.

PB (northwestern limb of syncline), followed to the southeast by an age reversal from PB through YD to B/A (southeastern limb of syncline/northwestern limb of anticline) and an upright sequence through YD to PB at the southeastern end (southeastern limb of anticline). The axes of the folds plunge towards the southwest at $\sim 20^\circ$ from the horizontal (Fig. 2).

The work presented in this study confirms this interpretation, provides more detail and expands the spatial scale. Figure 4 shows long transects spanning the entire syncline–anticline pair and ties these results to the records of Petrenko and others (2006). Figure 5 shows the BA–YD–PB sequence from the southeastern limb of the syncline. Figure 6 shows two high-resolution records from the northwestern limb of the syncline (LGM–OD–B/A), together with parallel transects, which are offset along the strike of the stratigraphy by meters to tens of meters.

In all climatic intervals sampled, Pâkitsoq $\delta^{15}\text{N}$ and $\delta^{18}\text{O}_{\text{atm}}$ values agree with GISP2 data within measurement errors. Consistent with previous observations (Petrenko and others, 2006), $\delta^{18}\text{O}_{\text{ice}}$ values in the Pâkitsoq transects are 1–2‰ higher (more ^{18}O -enriched) than in the GISP2 record.

This is probably due to differences in $\delta^{18}\text{O}$ of precipitation at the deposition sites of Pâkitsoq ice and Greenland Summit, caused by elevation and other factors. Pâkitsoq $[\text{CH}_4]$ values are mostly consistent with the GISP2 record, but some samples show elevated $[\text{CH}_4]$, commonly between 800 and 1400 ppb. With exceptions for $[\text{CH}_4]$, in all transects the characteristic values of ice and gas parameters for climatic intervals and the transitions between them are therefore consistent: (1) with values known from the Greenland Summit ice cores (Table 1); (2) between the various parameters (e.g. in a YD ice layer all parameters display YD values); and (3) between different profiles and sampling campaigns.

Figure 5 demonstrates the reproducibility achieved between different years in the same ice section. The figure combines five separate datasets spanning the YD–PB transition taken from 2001 to 2005, which show remarkable agreement. This demonstrates the suitability of Pâkitsoq ice for ongoing paleo-studies. Strictly speaking, the reproducibility applies to the values of the parameters, whereas the exact geographic location of a specific age horizon, i.e. its

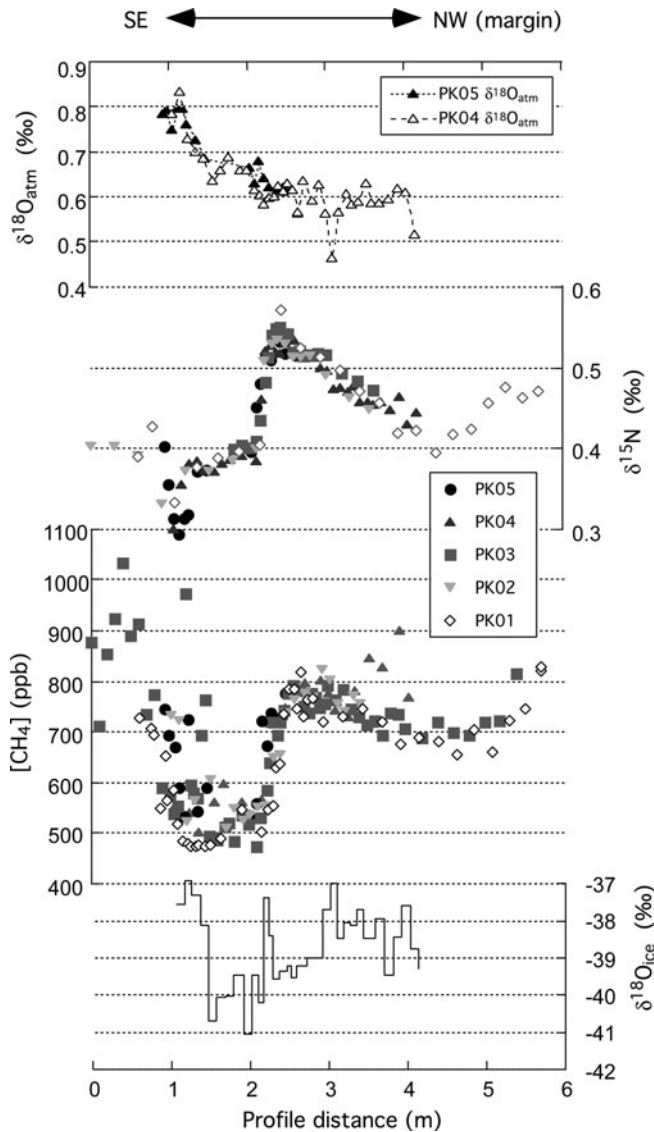


Fig. 5. Detailed ice and gas records of the YD–PB transition in Pâkitsoq ice. $\delta^{15}\text{N}$ and $[\text{CH}_4]$ records from five field seasons (2001–05, including PK04 TR and PK05 YD) show remarkable consistency. The gas parameters show the transition into the YD at the start (1 m) of the profile and the abrupt transition into the PB at ~ 2.3 m. $\delta^{18}\text{O}_{\text{atm}}$ records are from 2004 and 2005 and $\delta^{18}\text{O}_{\text{ice}}$ from 2004. The profiles have been aligned for the start of the $\delta^{15}\text{N}$ transition. Profile orientation (southeast–northwest) is reversed relative to Figure 4 to meet the convention of decreasing age towards the right.

profile distance, can vary as a function of ablation, dip of the ice layers and ice movement. Where necessary, we have adjusted the profile distances from different field seasons so that characteristic transitions match up. Such adjustments are in the order of tens of centimeters. This approach has limitations in cases where the layer width of age intervals varies as a result of differential thinning and proximity to fold axes. In such cases, not all transitions in two profiles can be aligned simultaneously, as can be seen for the $\delta^{18}\text{O}_{\text{ice}}$ profiles taken in 2003 and 2004 (Fig. 4). The slight shifts in profile distance of the climatic transitions observed between parallel profiles (i.e. offset along strike), or between profiles taken in the same nominal location in different years, are a result of the combination of ice movement and ablation as well as the three-dimensional geometry of the folds. However, these physical processes do not affect the

geochemical signals, so all profiles spanning the same stratigraphic layers show excellent agreement. This is analogous to ice-core records from sites with different accumulation rates the paleo-signals of which are still comparable. Therefore, field sampling at this site or similar sites requires the investigator to first establish the age relations along transects using diagnostic geochemical tracers prior to large-scale sampling.

Figure 6 shows a total of five sampling profiles from the 2004 and 2005 sampling seasons, centered on the OD–Bølling abrupt climatic transition. $[\text{CH}_4]$ rises from values below 500 ppb to between 600 and 700 ppb, associated with an excursion in $\delta^{15}\text{N}$ from $\sim 0.46\text{‰}$ to $\sim 0.62\text{‰}$. $\delta^{18}\text{O}_{\text{atm}}$ values about 1.1‰ indicate a gas age close to 15 ka BP, when $\delta^{18}\text{O}_{\text{atm}}$ reached its maximum (Bender and others, 1999; Severinghaus and others, 2006). Over the last glacial termination the combination of these values is unique for the OD–Bølling transition. Figure 6 also illustrates how the age–distance relationship changes substantially along strike. For example, PK05 TR and PK05 TR2 differ in the widths of the $[\text{CH}_4]$ transition and the $\delta^{15}\text{N}$ peak, which indicates varying degrees of thinning of ice layers with different proximity to the fold axis.

An additional test for the proposed folding and stratigraphy shown in Figure 4 is presented by a short transect (PK04 BAN), which is situated ~ 40 m northeast of the high-resolution sampling area (see Figs 2 and 3) in the southeastern limb of the syncline. $\delta^{18}\text{O}_{\text{atm}}$ exceeding 1.0‰ and $[\text{CH}_4]$ values clearly below 500 ppb (Fig. 6) are characteristic for LGM and OD. Towards the northwest, $[\text{CH}_4]$ rises coincident with a warming signal recorded in $\delta^{15}\text{N}$. This transect therefore spans the OD–Bølling transition as predicted by Petrenko and others (2006). The ice layers in this profile are more compressed than those in the PK04 BAS and PK05 TR profiles, as indicated by the very narrow $\delta^{15}\text{N}$ peak. The PK04 BAN profile is also valuable for establishing the overall geometry of ice layers because it provides two-dimensional spatial information in addition to the one-dimensional main transect lines. Together with the strike and dip of layers observed in the profiles (both directly and in the shift of reference points from year to year), we now have three-dimensional information on the Pâkitsoq stratigraphy confirmed by gas records.

Exposed interglacial ice of suspected Eemian origin

At the edge of the Pâkitsoq margin section there is a ~ 10 – 20 m wide layer of refrozen meltwater forming the so-called regelation ice, which is clear and bubble-free. Immediately adjacent there is a layer of ice from an interglacial period as indicated by visual appearance (clean light-colored ice surface containing abundant cryoconite holes) and relatively high $\delta^{18}\text{O}_{\text{ice}}$ ($\sim -32\text{‰}$; Reeh and others, 2002). According to the theory of ice flow at margins, this layer sequence should be older than those discussed in detail above and could therefore date to the Eemian interval, i.e. the last interglacial (Reeh and others, 1991). Because to date no ice cores in Greenland have captured the entire Eemian, a surface outcrop would be a unique opportunity to study this climate interval in the Northern Hemisphere. However, the transition to southeastern adjacent layers with full glacial $\delta^{18}\text{O}_{\text{ice}}$ values (-40‰) (28–32 m in Fig. 7) appears very abrupt, unlike the gradual onset of glacial conditions after the Eemian as recorded in Greenland Summit ice cores (NorthGRIP Members, 2004; Landais

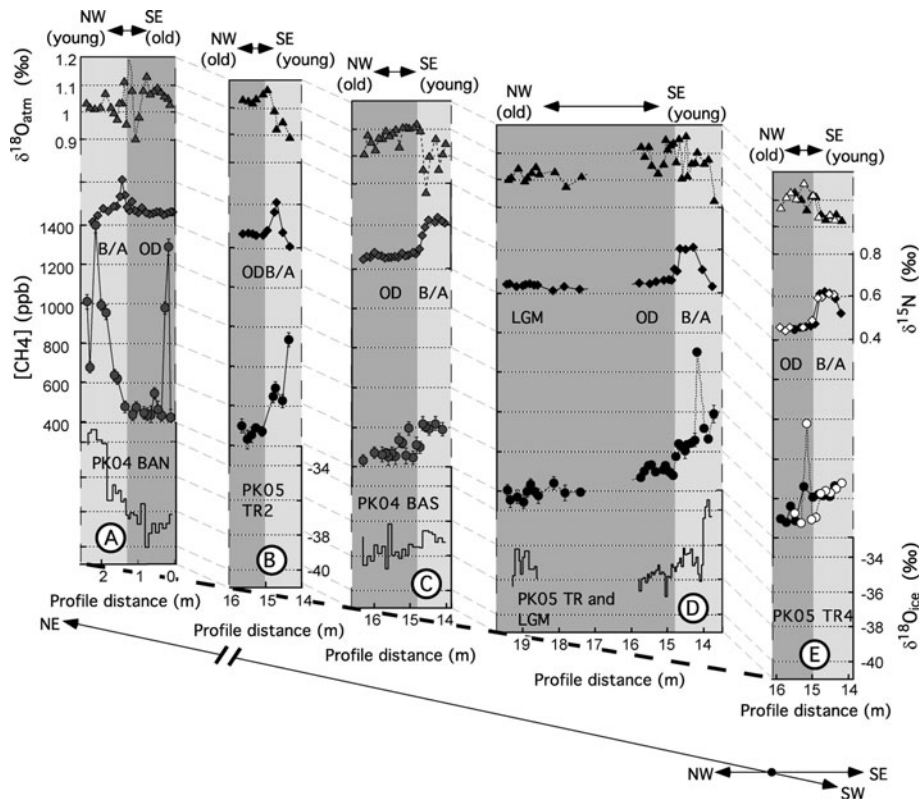


Fig. 6. Transition from the Oldest Dryas into the Bølling/Allerød as recorded in Pâkitsoq profiles. Four parallel profiles (panels B–E) are shown, and the same transition exposed in the opposite limb of the syncline to the northeast (panel A). The break in the northeast direction arrow indicates farther distance and switch across the syncline axis from the OD–Bølling transition in panel A. Grey symbols indicate data from 2004 samples; solid and open symbols are for data from 2005. Note the narrowing of the $\delta^{15}\text{N}$ peak from southwest to northeast in profiles E–B, indicating increasing thinning of the ice layers along strike. (A) PK04 BAN profile, located 38.5 m northeast (along the strike of the ice layers) of the PK02 reference pole (PK02 RP; Fig. 3). $[\text{CH}_4]$ data from this profile are field measurements. Samples collected at depth (z) ~ 0.3 m. (B) PK05 Tr2 profile, located 4.6 m to the southwest of PK02 RP; $z \sim 1.0$ m. (C) PK04 BAS profile, located 13 m southwest of PK02 RP; $z \sim 0.3$ m. (D) LGM, located ~ 27 m southwest of PK02 RP; $z \sim 1.1$ m. (E) Tr4 profile, located ~ 33 m to the southwest of PK02 RP. Open symbols for $z \sim 0.2$ m below the ice surface; solid symbols $z \sim 1.5$ m.

and others, 2006). In order to determine whether this sequence is indeed the post-Eemian glacial inception, as ice stratigraphy would suggest, or a different climate transition that has been emplaced by ice tectonics, we collected a 60 m long profile (PK05 MA) which was analyzed for our usual ice and gas parameters. The location of this profile is shown on Figure 3 and the data are presented in Figure 7.

A problem with this interpretation is that the YD $[\text{CH}_4]$ minimum is located further northwest, i.e. in younger ice, than the low $\delta^{18}\text{O}_{\text{ice}}$ values associated with the YD, while entrapped air is always contained in older ice. This reversal is likely due to distance scale discrepancies between the independently collected sample sets for $\delta^{18}\text{O}_{\text{ice}}$ and gas analyses. Although both transects followed the same line (marked by a tape measure), the different needs for each sample set (sample geometry, discrete vs continuous sampling) together with rough surface topography can lead to lateral offsets by up to ~ 2 m between the two sampling transects. From GPS measurements, the end-points of the gas and the ice profiles appear to be offset by 1.5 m (see position of points 5MA' and 5MA'' in Fig. 3), while nominally the profiles were the same length. Allowing for uncertainties of such magnitude, the datasets can be reconciled.

There are two other $\delta^{15}\text{N}$ peaks to the southeast (at 31 and 34 m) in ice with characteristics of the glacial period in $[\text{CH}_4]$ and $\delta^{18}\text{O}_{\text{ice}}$. The latter parameters show no variability associated with the $\delta^{15}\text{N}$ excursions, while $\delta^{18}\text{O}_{\text{atm}}$

stays about 0.5‰, which is too high for ice from the LGM. The combination of the four geochemical tracers southeast of 31 m is fairly close to YD values, which would suggest multiple folding of YD ice. We consider this possibility unlikely because $[\text{CH}_4]$ and $\delta^{18}\text{O}_{\text{atm}}$ values are consistently too low (both parameters are very robust regarding minimum values) and because of the wide spatial extent of this ice layer. Alternatively, the two $\delta^{15}\text{N}$ peaks at $\delta^{18}\text{O}_{\text{atm}} = \sim 0.5$ ‰ could indicate Dansgaard–Oeschger events 3 and 4 with ice ages between 23 and 25 ka BP (Fig. 1). In this case, the sequence would be missing the complete section of ice from the LGM. One possibility is that the LGM layer has been extremely thinned to form the $\delta^{18}\text{O}_{\text{ice}}$ minimum at 29 m (which is interpreted in the previous paragraph and Fig. 7 as YD). This would resolve the ice-age–gas-age contradiction discussed above, but raises the question as to the nature of the 30 m $\delta^{18}\text{O}_{\text{ice}}$ maxima (sequence reversal to the BA or interstadial). The possible occurrence of interstadial events in this section is an exciting prospect for future work in Pâkitsoq, but with the available records we cannot resolve the contradicting evidence and confirm unequivocally the nature of the features between 31 and 35 m. Given that $\delta^{18}\text{O}_{\text{ice}}$ values are averaged over 20 cm and the gas data spot-sampled every 50 cm, the records may miss short-lived events or strongly thinned sections that are necessary to resolve the stratigraphy of these layers.

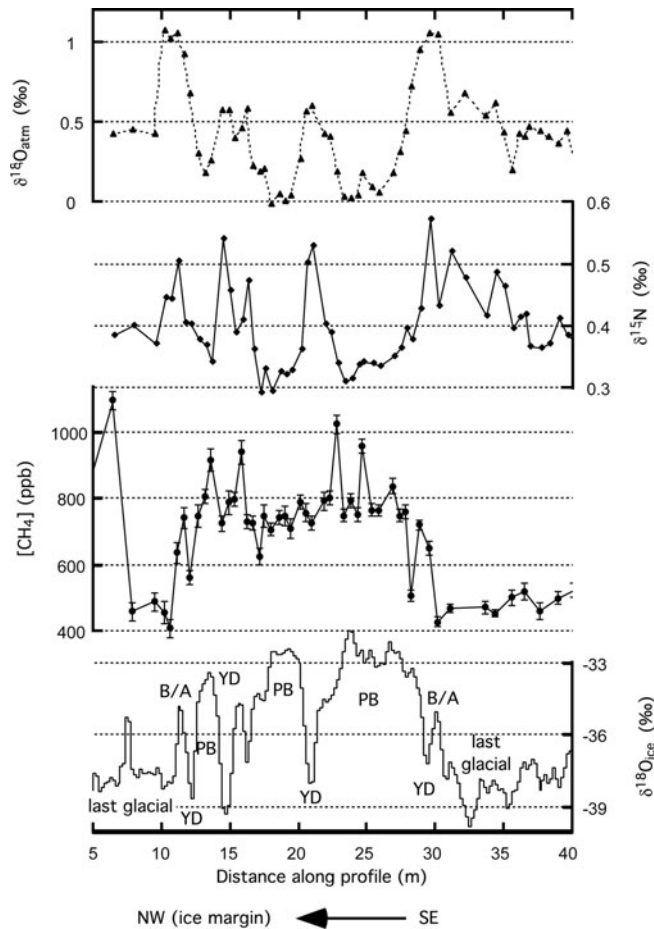


Fig. 7. Margin transect (PK05 MA) revealing suspected Eemian ice as dating to LGM and TI. The glacial–interglacial transition at ~ 30 m, as seen in $\delta^{18}\text{O}_{\text{ice}}$, is associated with a positive excursion in $\delta^{15}\text{N}$ (at ~ 29.5 m), which marks it as a glacial termination and not an inception. The $[\text{CH}_4]$ minimum at 27 m indicates the YD and identifies the sequence as TI. The multiply repeated successions of climatic periods from YD to LGM between 5 and 17 m are not resolved in sufficient detail in the gas records, so the presented interpretation of events remains speculative. Note that for this profile, distance increases towards the southeast, in contrast to all other presented transects.

Despite the uncertainties discussed, the sequence is undoubtedly a glacial termination and there is no other glacial–interglacial transition between it and the main study area where TI is exposed (as suggested by $\delta^{18}\text{O}$ ice profiles from Reeh and others (2002) and surface ice appearance; Fig. 2). Therefore, the margin profile is most likely the far limb of a large anticline exposing once more the transition from the last glacial into the Holocene. The only other possible scenario requires that an entire sequence of Eemian ice be missing from the profile while a second outcrop of the Eemian period (sampled by the PK05 MA profile) be overturned. This would require two fault zones, as opposed to a simple fold. In fact, the large-scale anticline postulated by the first, simpler, interpretation can be seen in aerial view (Fig. 2), where in the upper right-hand section lighter-colored Holocene ice wraps around the darker ice section of the glacial period.

Moving further to the northwest along the profile shown in Figure 7, with decreasing profile distance, several more layers with low $\delta^{18}\text{O}_{\text{ice}}$ appear between 13 and 25 m. We speculate that these are multiple outcrops of YD ice, alternating with PB ice in a series of accordion-type folds

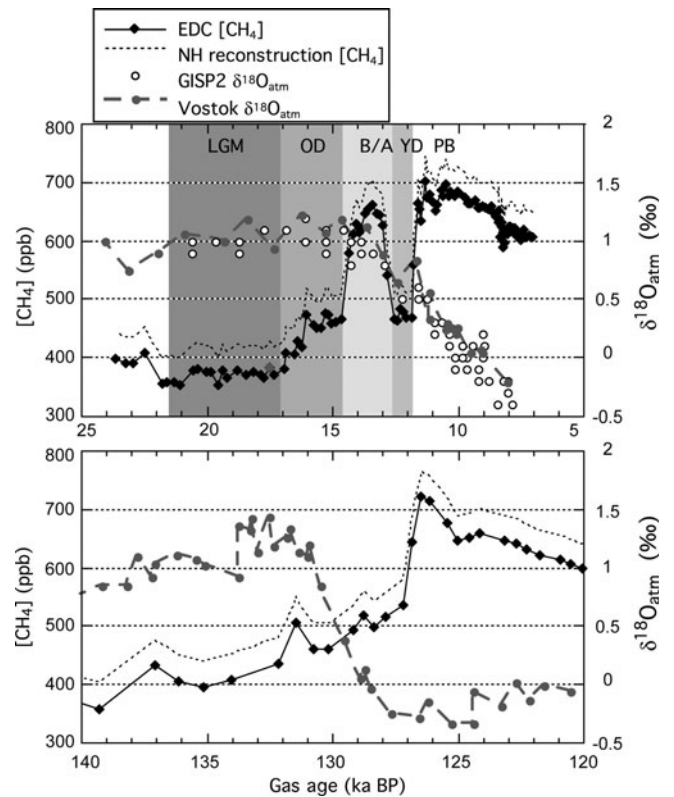


Fig. 8. Comparison of $[\text{CH}_4]$ and $\delta^{18}\text{O}_{\text{atm}}$ over (a) TI and (b) TII. EPICA $[\text{CH}_4]$ data are from R. Spahni and T. Stocker (<http://doi.pangaea.de/10.1594/PANGAEA.472484>). A reconstruction of $[\text{CH}_4]$ for the Northern Hemisphere based on these data was made following Suwa and others (2006) to make the record comparable to Figure 1. Comparison of $\delta^{18}\text{O}_{\text{atm}}$ data for Vostok from M. Bender and M. Suwa (<http://nsidc.org/data/nsidc-0311.html>) and from GISP2 TI from Bender and others (1994) shows that this parameter is truly a global signal.

until ice from the last glacial period is reached again at 10 m. The low sampling resolution does not permit unequivocal identification of the complete sequence. However, the individual events display the characteristics of the YD–PB transition with $\delta^{18}\text{O}_{\text{atm}}$ between 0.55‰ and 0.60‰ (never reaching full glacial values between 12 and 28 m) and associated $\delta^{15}\text{N}$ peaks. This is consistent with our interpretation regarding the age of each event. Consequently, this adds further support to the conclusion that the whole sequence is indeed TI, with its distinct and geochemically well-characterized climatic events.

Although the complicated folding makes it difficult to rule out beyond doubt that the sequence represents TII, the ensemble of stratigraphic and geochemical evidence is clearly easier to reconcile with a TI sequence. These results therefore imply that no Eemian ice is available for paleo-studies at Pâkitsoq. However, the results are important for understanding the large-scale three-dimensional structure of the ice layers, to be reported elsewhere by Reeh and others. Whereas previously we have demonstrated folding at Pâkitsoq on the scale of tens of meters, this study shows that the complete ice-margin sequence contains one large anticline that spans several hundred meters.

Early-Holocene climate oscillations

We targeted new objectives for paleo-studies during the 2005 field season. While to the northwest of the main study

area the individual Dansgaard–Oeschger events of the last glacial period would be extremely difficult to identify in the complexly folded Pâkitsoq sequence, to the southeast the early part of the Holocene appears less folded and has several promising targets. The most obvious is the cold event centered on 8.2 ka BP (hereafter referred to as 8.2k). The cooling is evident in climate records from a large range of geographic locations (Alley and others, 1997) and may provide important clues to climate system dynamics in the postglacial period. Importantly, the GISP2 8.2k record contains easily identified characteristic signals in $[\text{CH}_4]$, $\delta^{15}\text{N}$ and $\delta^{18}\text{O}_{\text{ice}}$ (Kobashi and others, 2007) that should facilitate its identification at Pâkitsoq.

The $\delta^{18}\text{O}_{\text{ice}}$ profile from a study in 1988 shows a marked dip in an early-Holocene section that possibly indicates the 8.2k event (fig. 4b of Reeh and others, 2002). That profile was taken several hundred meters to the north of our sampling transects, making it logistically difficult to work in the exact location. Also, ablation removed $\sim 40\text{ m}$ of ice between 1988 and 2005, preventing direct comparison. To locate the 8.2k event closer to the main study area, we used estimates from an ice-flow model, to be published elsewhere by Reeh and others, to account for lateral offset, ice movement and ablation since the 1988 survey. A $\sim 130\text{ m}$ long profile for $\delta^{18}\text{O}_{\text{ice}}$ (PK05 C-profile) and a 40 m long gas profile (PK05 EH) centered on the projected 8.2k location were collected (Figs 2 and 3 for location, Fig. 9 for records). $\delta^{18}\text{O}_{\text{ice}}$ reveals the southeastward transition from the LGM/OD (130 m) through the YD (110 m) and the PB oscillation ($\sim 105\text{ m}$) into the PB and early Holocene. The $[\text{CH}_4]$ record of the gas profile mostly exceeds any pre-industrial values measured in GISP2 and is therefore not shown. The likely cause is surface contamination, as these samples were collected only 20 cm beneath the ice surface (instead of the usual $>50\text{ cm}$). As a consequence, $[\text{CH}_4]$ does not provide useful age information. Apart from two outliers contaminated by meltwater (as indicated by abnormally high O_2/N_2 and Ar/N_2 ratios), $\delta^{18}\text{O}_{\text{atm}}$ shows a decline from 0.0‰ to -0.1‰ (Fig. 9). Such values occur between 9 and 10 ka BP, according to the high-precision $\delta^{18}\text{O}_{\text{atm}}$ record from Siple Dome, Antarctica (Severinghaus and others, 2006). Interestingly, at the north-westernmost part of the gas profile ($\sim 73\text{ m}$), $\delta^{15}\text{N}$ rises from $\sim 0.26\text{‰}$ to $\sim 0.3\text{‰}$, consistent with the recovery from a cold event. Indeed, $\delta^{18}\text{O}_{\text{ice}}$ shows a minimum, i.e. a short-lived cold event, recorded in two adjacent samples just southeast of the $\delta^{15}\text{N}$ rise (at $\sim 72\text{ m}$). The direction of the offset between the $\delta^{15}\text{N}$ and $\delta^{18}\text{O}_{\text{ice}}$ signals is consistent with the expected ice-age–gas-age offset. During the time frame set by $\delta^{18}\text{O}_{\text{atm}}$, there is a distinct cooling event of about -2°C recorded in GISP2 at 9.3 ka BP (hereafter 9.3k) associated with a dip in $\delta^{18}\text{O}_{\text{ice}}$ by $\sim 1.1\text{‰}$ (Stuiver and others, 1995) and in $\delta^{15}\text{N}$ by $\sim 0.02\text{--}0.03\text{‰}$ (Kobashi, 2007; Kobashi and others, 2008). In comparison, the excursions in our profile are somewhat larger, with $\sim 1.5\text{‰}$ for $\delta^{18}\text{O}_{\text{ice}}$ and at least 0.04‰ for $\delta^{15}\text{N}$. A larger $\delta^{18}\text{O}_{\text{ice}}$ transition signal in Pâkitsoq compared with GISP2 is also observed for the YD event (Petrenko and others, 2006), supporting our 9.3k interpretation for the excursion at 72 m. Unfortunately, the event is captured by only one gas data point at the very end of our profile so that its temporal structure and absolute magnitude remain unresolved. However, $\delta^{15}\text{N}$ is a very robust parameter and the elemental ratios for O_2 , N_2 and Ar (data not shown) prove that the value is not affected by melt contamination. Therefore, the signal indicates a real climatic excursion. The

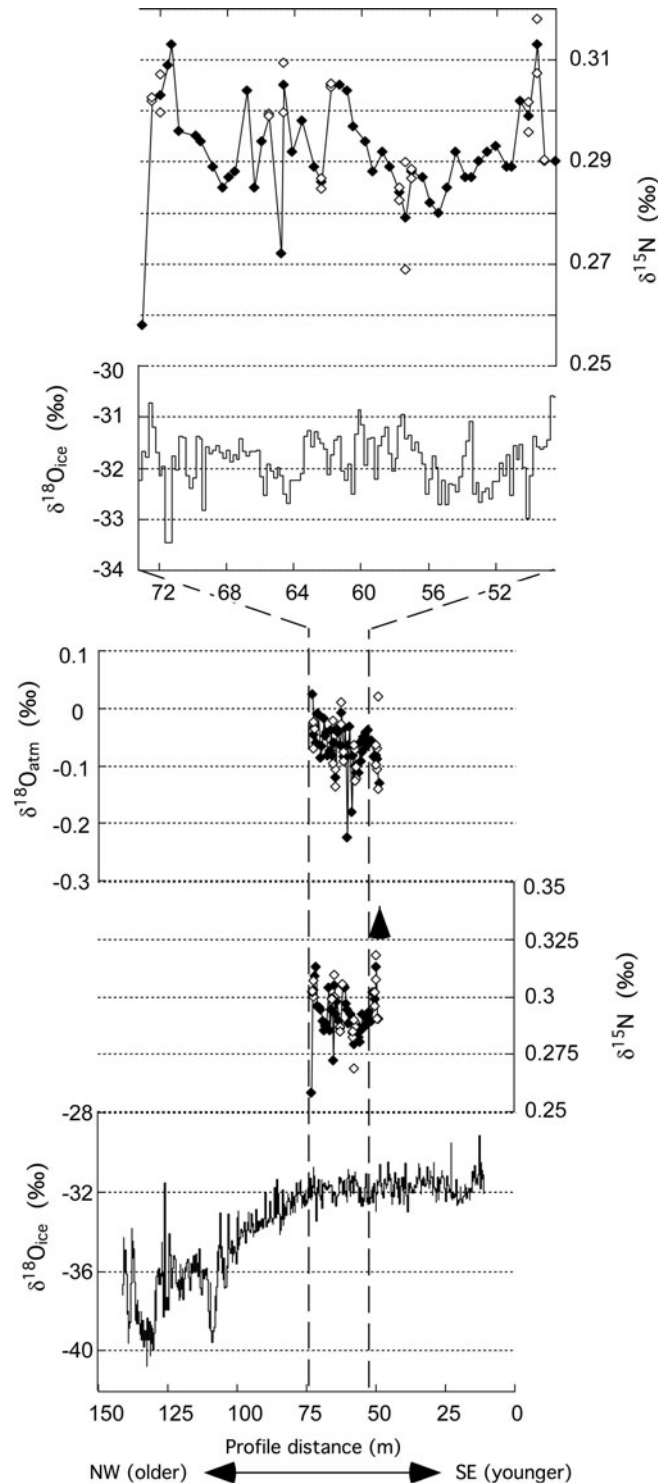


Fig. 9. Pâkitsoq records covering the early Holocene (PK05 EH and PK05-C profiles). The $\delta^{18}\text{O}_{\text{ice}}$ profile (2005 C-profile) shows the last glacial termination (100–140 m) to the early Holocene (0–100 m). $\delta^{18}\text{O}_{\text{atm}}$ values are indicative of an age of 9–10 ka BP for the length of the gas sample profile (PK05 EH, $\sim 50\text{--}75\text{ m}$). The low northwesternmost $\delta^{15}\text{N}$ value (see inset) indicates abrupt cooling, most likely the 9.3 ka BP cold event. Open symbols indicate individual results of duplicate measurements. Arrow indicates a single outlier in $\delta^{15}\text{N}$ (off scale) caused by melting of the sample.

PK05 EH profile stopped short of the ice containing the 8.2k event, which would be found by extending this transect to the southeast in potential future work. However, the likely finding of the 9.3k event demonstrates the potential of the Pâkitsoq site for studies of early-Holocene climate instability.

CONCLUSIONS

Following earlier work at the Pâkitsoq ice margin presented by Petrenko and others (2006), we use the same combination of geochemical parameters in ice and gas phases ($\delta^{18}\text{O}_{\text{ice}}$, $\delta^{18}\text{O}_{\text{atm}}$, $\delta^{15}\text{N}$ and $[\text{CH}_4]$) to confirm the stratigraphic interpretation of the study's main transect as a multiply folded sequence including ice strata from the last glacial period into the early Holocene. While previous work focused on the identification of the YD cold interval, we can now identify all TI climatic intervals, including LGM, Oldest Dryas, Bølling/Allerød, Younger Dryas and Preboreal. The exact location of climatic transitions in the ice is slightly variable from year to year due to melting and ice-flow processes. Nevertheless, the geochemical tracer records spanning the same stratigraphic layers can be reproduced extremely well between different field seasons. Profiles taken in parallel, i.e. offset along the strike of the ice layers, confirm the pattern of climatic boundaries in the ice predicted by visual inspection from the air and the original mapping of the fold structure (Petrenko and others, 2006). They also provide additional information in the third dimension.

Two profile lines extend the spatial coverage of the Pâkitsoq gas records and reveal further stratigraphic features. Towards the northwest, warm-period ice at the very margin does not appear to date to the Eemian, the penultimate Interglacial, as was expected from principles of ice flow. Instead, our geochemical profiles show that it is most likely a repeated sequence of Holocene to Late-glacial period ice in reverse layering. This ice forms the northwestern limb of an anticline spanning several hundred meters, the southeastern limb of which exposes the sequence again in the main study area. Folds of this magnitude previously have not been resolved at Pâkitsoq. The central part of this anticline exposes ice from the last glacial period. Towards the southeast, we extend our profiles into early-Holocene ice and find evidence of the climatic instability during the 9.3k cold event. With this study, we have established targets for paleo-investigations at Pâkitsoq that range from full glacial conditions through the climate reversals at the end of the last ice age to the fluctuations of the early Holocene, all with an essentially unlimited supply of ice.

This work further confirms that $\delta^{18}\text{O}_{\text{ice}}$, $\delta^{15}\text{N}$ and $\delta^{18}\text{O}_{\text{atm}}$ records in Pâkitsoq ice are well preserved. More than in our preceding work, however, we find that $[\text{CH}_4]$ in the ice can be subject to alterations. A correlation between sampling depth and degree of contamination is evident, and the patterns of contamination and implications for paleo-studies will be discussed in detail elsewhere by Schaefer and others. However, the vast majority of $[\text{CH}_4]$ measurements in our high-resolution profiles show good agreement with GISP2 values. Also, even a sensitive parameter like $\delta^{13}\text{CH}_4$ measured in Pâkitsoq ice agrees well with data from GISP2 ice (Schaefer and others, 2006; Sowers, 2006) and reasonably well with an Antarctic record (Fischer and others, 2008). Pâkitsoq is a suitable and promising site for paleo-studies of trace constituents in the ice and occluded air for all climatic intervals since the LGM.

ACKNOWLEDGEMENTS

We thank J. Chappellaz for steering us to the Pâkitsoq site and R. Keeling for helpful discussions. We also thank P. Rose, N. Ness, K. Ranke, D. Ricke, M. Arsenault, A. Ahlstrøm,

A. Munk Solgaard and L. Rangvid for support in the field, and J. Ahrens and R. Beaudette for laboratory assistance. M. Suwa and an anonymous reviewer were very helpful in improving the manuscript. VECO Polar Resources provided excellent logistical support. The 109th Airlift Wing provided transport of personnel and gear to and from Greenland. We thank the Glaciology Group, Niels Bohr Institute, University of Copenhagen, for performing the $\delta^{18}\text{O}_{\text{ice}}$ measurements. Ice Coring and Drilling Services continuously improved our sample drill. We thank the Danish Polar Center and Greenland Home Rule for permission to carry out this research. This work was funded by US National Science Foundation grants OPP0221470 (J.P.S.) and OPP0221410 (E.J.B.), by a Packard Fellowship (J.P.S.), Canadian Foundation for Climate and Atmospheric Sciences grant MAMMOTH (J.R.M.), American Chemical Society grant PRF 42551-AC2 (H.S. and E.J.B.) and by Danish Research Council grant 21-02-0504 (N.R.).

REFERENCES

- Aciego, S.M., K.M. Cuffey, J.L. Kavanaugh, D.L. Morse and J.P. Severinghaus. 2007. Pleistocene ice and paleo-strain rates at Taylor Glacier, Antarctica. *Quat. Res.*, **68**(3), 303–313.
- Alley, R.B., P.A. Mayewski, T. Sowers, M. Stuiver, K.C. Taylor and P.U. Clark. 1997. Holocene climatic instability: a prominent, widespread event 8200 yr ago. *Geology*, **25**(6), 483–486.
- Bender, M. and 6 others. 1994. Climate correlations between Greenland and Antarctica during the past 100,000 years. *Nature*, **372**(6507), 663–666.
- Bender, M., B. Malaize, J. Orcharo, T. Sowers and J. Jouzel. 1999. High precision correlations of Greenland and Antarctic ice core records over the last 100 kyr. In Clark, P.U., R.S. Webb and L.D. Keigwin, eds. *Mechanisms of global climate change at millennial time scales*. Washington, DC, American Geophysical Union.
- Brook, E.J., S. Harder, J. Severinghaus, E.J. Steig and C.M. Sucher. 2000. On the origin and timing of rapid changes in atmospheric methane during the last glacial period. *Global Biogeochem. Cycles*, **14**(2), 559–572.
- Fischer, H. and 10 others. 2008. Changing boreal methane sources and constant biomass burning during the last termination. *Nature*, **452**(7189), 864–867.
- Fronval, T. and E. Jansen. 1996. Rapid changes in ocean circulation and heat flux in the Nordic seas during the last interglacial period. *Nature*, **383**(6603), 806–810.
- Gouzy, A., B. Malaizé, C. Pujol and K. Charlier. 2004. Climatic 'pause' during Termination II identified in shallow and intermediate waters off the Iberian margin. *Quat. Sci. Rev.*, **23**(14–15), 1523–1528.
- Grootes, P.M. and M. Stuiver. 1997. Oxygen 18/16 variability in Greenland snow and ice with 10^3 to 10^5 -year time resolution. *J. Geophys. Res.*, **102**(C12), 26,455–26,470.
- Kobashi, T. 2007. Greenland temperature, climate change, and human society during the last 11,600 years. (PhD thesis, University of California, San Diego.)
- Kobashi, T., J.P. Severinghaus, E.J. Brook, J.-M. Barnola and A.M. Grachev. 2007. Precise timing and characterization of abrupt climate change 8200 years ago from air trapped in polar ice. *Quat. Sci. Rev.*, **26**(9–10), 1212–1222.
- Kobashi, T., J.P. Severinghaus and K. Kawamura. 2008. Argon and nitrogen isotopes of trapped air in the GISP2 ice core during the Holocene epoch (0–11,500 B.P.): methodology and implications for gas loss processes. *Geochim. Cosmochim. Acta*, **72**(19), 4675–4686.
- Landais, A., J.P. Steffensen, N. Caillon, J. Jouzel, V. Masson-Delmotte and J. Schwander. 2004. Evidence for stratigraphic distortion in the Greenland Ice Core Project (GRIP) ice core

- during Event 5e1 (120 kyr BP) from gas isotopes. *J. Geophys. Res.*, **109**(D6), D06103. ([10.1029/2003JD004193](https://doi.org/10.1029/2003JD004193).)
- Landais, A. and 8 others. 2006. The glacial inception as recorded in the NorthGRIP Greenland ice core: timing, structure and associated abrupt temperature changes. *Climate Dyn.*, **26**(2–3), 273–284.
- Loulergue, L. and 9 others. 2008. Orbital and millennial-scale features of atmospheric CH₄ over the past 800,000 years. *Nature*, **453**(7193), 383–386.
- North Greenland Ice Core Project (NorthGRIP) Members. 2004. High-resolution record of Northern Hemisphere climate extending into the last interglacial period. *Nature*, **431**(7005), 147–151.
- Petit, J.R. and 18 others. 1999. Climate and atmospheric history of the past 420,000 years from the Vostok ice core, Antarctica. *Nature*, **399**(6735), 429–436.
- Petrenko, V.V. 2008. A study of carbon-14 of paleoatmospheric methane for the last glacial termination from ancient glacial ice. (PhD thesis, University of California San Diego.)
- Petrenko, V.V., J.P. Severinghaus, E.J. Brook, N. Reeh and H. Schaefer. 2006. Gas records from the West Greenland ice margin covering the Last Glacial Termination: a horizontal ice core. *Quat. Sci. Rev.*, **25**(9–10), 865–875.
- Petrenko, V.V. and 11 others. 2009. ¹⁴CH₄ measurements in Greenland ice: investigating last glacial termination CH₄ sources. *Science*, **324**(5924), 506–509.
- Price, P.B. 2007. Microbial life in glacial ice and implications for a cold origin of life. *FEMS Microbiol. Ecol.*, **59**(2), 217–231.
- Reeh, N. and H.H. Thomsen. 1994. Introduction to the Paakitsoq 1994 field programme. In Thomsen, H.H. and N. Reeh, eds. *Field report of paleo-environmental studies at the Greenland ice sheet margin, Paakitsoq, West Greenland*. Copenhagen, Grønlands Geologiske Undersøgelse. (Rapport 94/15.)
- Reeh, N., H. Oerter, A. Letrégouilly, H. Miller and H.W. Huberten. 1991. A new, detailed ice-age oxygen-18 record from the ice-sheet margin in central West Greenland. *Palaeogeogr., Palaeoclimatol., Palaeoecol.*, **90**(4), 373–383.
- Reeh, N., H. Oerter and H. Miller. 1993. Correlation of Greenland ice-core and ice-margin δ(¹⁸O) records. In Peltier, W.R., ed. *Ice in the climate system*. Berlin, etc., Springer-Verlag, 481–497. (NATO ASI Series I: Global Environmental Change 12.)
- Reeh, N., H. Oerter and H.H. Thomsen. 2002. Comparison between Greenland ice-margin and ice-core oxygen-18 records. *Ann. Glaciol.*, **35**, 136–144.
- Sánchez-Goñi, M.F., F. Eynaud, J.L. Turon and N.J. Shackleton. 1999. High resolution palynological record off the Iberian margin: direct land–sea correlation for the Last Interglacial complex. *Earth Planet. Sci. Lett.*, **171**(1), 123–137.
- Schaefer, H., M.J. Whiticar, E.J. Brook, V.V. Petrenko, D.F. Ferretti and J.P. Severinghaus. 2006. Ice record of ¹³C for atmospheric CH₄ across the Younger Dryas–Preboreal transition. *Science*, **313**(5790), 1109–1112.
- Schwander, J., T. Sowers, J.M. Barnola, T. Blunier, A. Fuchs and B. Malaizé. 1997. Age scale of the air in the Summit ice: implication for glacial–interglacial temperature change. *J. Geophys. Res.*, **102**(D16), 19,483–19,493.
- Severinghaus, J.P. and E.J. Brook. 1999. Abrupt climate change at the end of the last glacial period inferred from trapped air in polar ice. *Science*, **286**(5441), 930–934.
- Severinghaus, J.P., T. Sowers, E.J. Brook, R.B. Alley and M.L. Bender. 1998. Timing of abrupt climate change at the end of the Younger Dryas interval from thermally fractionated gases in polar ice. *Nature*, **391**(6663), 141–146.
- Severinghaus, J.P., R. Beaudette and E.J. Brook. 2006. Millennial-scale variations in oxygen-18 of atmospheric molecular oxygen. [Abstr. U34B-01.] *Eos*, **87**(52), Fall Meet. Suppl.
- Souchez, R., M. Lemmens and J. Chappellaz. 1995. Flow-induced mixing in the GRIP basal ice deduced from the CO₂ and CH₄ records. *Geophys. Res. Lett.*, **22**(1), 41–44.
- Sowers, T.A. 2006. Methane isotope records spanning the last 160kyr: correlations and conundrums. [Abstr. U33C-04.] *Eos*, **87**(52), Fall Meet. Suppl.
- Stuiver, M., P.M. Grootes and T.F. Braziunas. 1995. The GISP2 δ¹⁸O climate record of the past 16,500 years and the role of the Sun, ocean and volcanoes. *Quat. Res.*, **44**(3), 341–354.
- Suwa, M., J.C. von Fischer, M.L. Bender, A. Landais and E.J. Brook. 2006. Chronology reconstruction for the disturbed bottom section of the GISP2 and the GRIP ice cores: implications for Termination II in Greenland. *J. Geophys. Res.*, **111**(D2), D02101. ([10.1029/2005JD006032](https://doi.org/10.1029/2005JD006032).)
- Wilch, T.I., W.C. McIntosh and N.W. Dunbar. 1999. Late Quaternary volcanic activity in Marie Byrd Land: potential ⁴⁰Ar/³⁹Ar-dated time horizons in West Antarctic ice and marine cores. *Geol. Soc. Am. Bull.*, **111**(10), 1563–1580.

MS received 21 July 2008 and accepted in revised form 28 December 2008